Available online at www.sciencedirect.com
ScienceDirect
Journal of Power Sources 165 (2007) 108–113
JOURNAL OF POWER SOURCES
www.elsevier.com/locate/jpowsour

Short communication

A novel methanol-tolerant Ir-Se chalcogenide electrocatalyst for oyxgen reduction

Kunchan Lee, Lei Zhang, Jiujun Zhang *

Institute for Fuel Cell Innovation, National Research Council of Canada, 4250 Wesbrook Mall, Vancouver, BC, Canada V6T 1W5

Received 17 October 2006; received in revised form 28 November 2006; accepted 29 November 2006
Available online 12 January 2007

Abstract

A novel methanol-tolerant oxygen-reduction catalyst, Iridium-selenium (Ir-Se) chalcogenide, was synthesized by chemical precipitation in an organic solvent. Auger electron spectroscopy (AES) analysis confirmed that the synthesized Ir-Se chalcogenide had a chemical formula of Ir_4Se. This chalcogenide showed strong catalytic activity towards the oxygen reduction reaction (ORR) and a high methanol tolerance. It was found that most of the oxygen could be directly reduced to water through a four-electron pathway with less than 10% hydrogen peroxide (H_2O_2) being produced during the ORR. The improvement in catalytic activity of the Ir-Se chalcogenide in comparison with that of pure Ir might be attributed to the effect of a bimetallic interaction.

Keywords: Chalcogenide; Iridium; Selenium; Electrocatalyst(s); Oxygen reduction reaction; Methanol tolerance

1. Introduction

Direct methanol fuel cells (DMFCs) are considered to be possible for fuel cell commercialization due to their easy fuel distribution and storage and the high-energy density of their methanol fuel. However, at least two major challenges need to be overcome for commercialization: high cost and low performance. Methanol (MeOH) crossover is a major cause of the low performance. MeOH permeating from the anode to the cathode through the membrane reacts directly with the cathode catalyst and O_2 to decrease the cathode potential and so reduce fuel efficiency. Therefore, a cathode catalyst which is inert to MeOH is highly desirable. The platinum (Pt)-based catalysts currently used as state-of-the-art cathode electrocatalysts have a high cost and a low oxygen reduction reaction (ORR) selectivity in the presence of MeOH. Developing a cathode catalyst which is both MeOH-tolerant and cost effective is a priority for DMFC research and development.

For many years, tremendous effort has been invested in developing novel electrocatalysts with a high ORR activity and methanol tolerance [1–3]. In particular, ruthenium (Ru)-based chalcogenides have shown a high ORR activity and MeOH tolerance in acidic media. In these chalcogenide catalysts, the active catalytic center has been identified as metallic Ru. It is also known that the chalcogen-like selenium (Se) in the catalyst can prevent the metallic Ru from forming Ru-oxides, thereby resulting in an enhanced ORR catalytic activity [4]. However, the catalytic activity of Ru-based catalysts is still not high enough for practical application in DMFCs.

Iridium (Ir) is one of the most stable metals among Pt-group metals in acidic media [5]. Although Ir has a much lower activity towards ORR than does Pt, it is interesting to note that its activity towards MeOH oxidation is also lower than that of Pt [6–8]. The surfaces of Ir have a strong affinity for OH or O species, forming a surface with a high oxide coverage even at a low potential. The formation of Ir-oxide is probably responsible for the low ORR activity [5,9–11]. From the viewpoint of catalyst design, modification of Ir could be a feasible approach to the improvement of the catalytic properties.

Based on these considerations, the research presented in this paper synthesized a novel Ir-Se chalcogenide as an alternative catalyst for the DMFC cathode reaction. The chemical structure of the synthesized Ir-Se chalcogenide was analyzed by Auger electron spectroscopy analysis. The catalytic activities towards methanol oxidation and oxygen reduction were investigated.

* Corresponding author. Tel.: +1 604 221 3087
E-mail address: jiujun.zhang@nrc.gc.ca (J. Zhang).

0378-7753/$ – see front matter © 2006 Elsevier B.V. All rights reserved.
doi:10.1016/j.jpowsour.2006.11.063

2. Experimental

2.1. Catalyst synthesis

The Ir-Se chalcogenide catalyst was synthesized by a chemical precipitation reaction between Ir carbonyl(dodecacarbonyltetrairidium: $Ir_4(CO)_{12}$, Alpha) and Se (powder, Alpha) in xylene solvent [12]. The xylene solvent was bubbled with argon for over 30 min to remove dissolved oxygen before the Se powder was added. Next, the xylene under reflux was heated to 140 °C for 30 min and then cooled to room temperature. The Ir carbonyl was added to this xylene reflux, which was then heated to 130–140 °C. All procedures were performed under argon with stirring. After being heated for over 20 h, the refluxing liquid was cooled and the precipitates were filtered and then washed with diethylether.

2.2. Electrode preparation

Electrochemical measurements were taken using a rotating glassy carbon disk-platinum ring electrode (RRDE). The catalyst ink, prepared according to Schmidt's report [13], was applied manually to the glassy carbon disk surface. For comparison, Pt/C (20 wt.%, E-TEK) and Ir/C (20 wt.%, E-TEK) catalysts were coated on the electrode surface in the same way. The loadings for Ir-Se chalcogenide and carbon-supported catalysts were 61 and 73 $\mu g cm^{-2}$, respectively. A reversible hydrogen electrode (RHE) and Pt wire were used as the reference and the counter electrodes, respectively. Aqueous solutions of 0.5 M H_2SO_4 with and without methanol (MeOH) were used as the electrolytes. All reported current densities were expressed versus geometric surface area of the disk electrode. All electrochemical experiments were carried out at 25 °C and ambient pressure.

2.3. Collection efficiency of RRDE

For H_2O_2 collection experiments, the electrode was prepared as described above. The electrolyte was deaerated 0.1 M NaOH containing 10 mM $K_3Fe(CN)_6$ [13]. The potential scan rate for the disk electrode was 5 $mV s^{-1}$, and a constant potential at 1.2 V versus RHE was applied to the ring electrode. At this ring potential, the oxidation of $[Fe(CN_6)]^{4-}$, which is produced at the disk electrode, to $[Fe(CN)_6]^{3-}$ proceeds under pure diffusion control. The collection efficiency, N, was then determined from the ring (I_R) and disk (I_D) currents according to the following equation: $N = -I_R/I_D$. The obtained collection efficiency was 0.19.

2.4. Physical characterization of the Ir-Se chalcogenide catalyst

Auger electron spectroscopy (AES) was carried out using a Microlab 350 system (Thermo Electron Corp.) equipped with a field emission source (10 keV, 2 nA) and hemispherical energy analyzer. In order to avoid charging problems during AES analysis, sample powder was dispersed on 0.5 cm × 0.5 cm indium foil prior to being analyzed. The morphology of the synthesized chalcogenide samples was confirmed by high-resolution transmission electron microscope (HR-TEM: FEI TECNAI G^2).

3. Results and discussion

3.1. Physical characterization

For the morphology of the synthesized Ir-Se chalcogenide powder, TEM measurements were carried out, as shown in Fig. 1. It can be seen that the powder consists of nano-clusters of 100–200 nm. Within the nano-clusters, nano-particles of 4–5 nm can be clearly observed.

In order to probe the surface compositions and characterization of the nano-particles, an AES surface analysis was used. Fig. 2(a) shows the Auger spectra for the powder. The peaks for Ir MNN, Se LMM, C KLL, and O KLL transitions are indicative of the co-existence of Ir and Se, suggesting that the particle is Ir-Se chalcogenide. In the Auger spectrum of Ir MNN, shown in Fig. 2(b), the kinetic energy (KE) of the Ir peak is at 1978.3 eV, indicating that the chemical state of Ir is slightly different from the metallic-like state of pure Ir at 1977.8 eV [14]. In contrast, the peaks of Se LMM show a large chemical shift of 2.2 from 1306.9 to 1309.1 eV compared to that of high-purity Se [15,16]. Such a large chemical shift to positive KE in the Se LMM transitions might be a result of charge transfer from Ir to Se after the formation of Ir-Se bonding. Therefore, the AES analysis confirmed that Ir-Se chalcogenide was obtained in our synthesis process. In addition, there was no observation of any Ir and Se oxides-associated shape change or chemical shift on the Auger peaks. This suggests that the surface of Ir-Se chalcogenide might be stable in air.

Table 1 shows the surface chemical composition of synthesized Ir-Se chalcogenide powder obtained by AES analysis. The

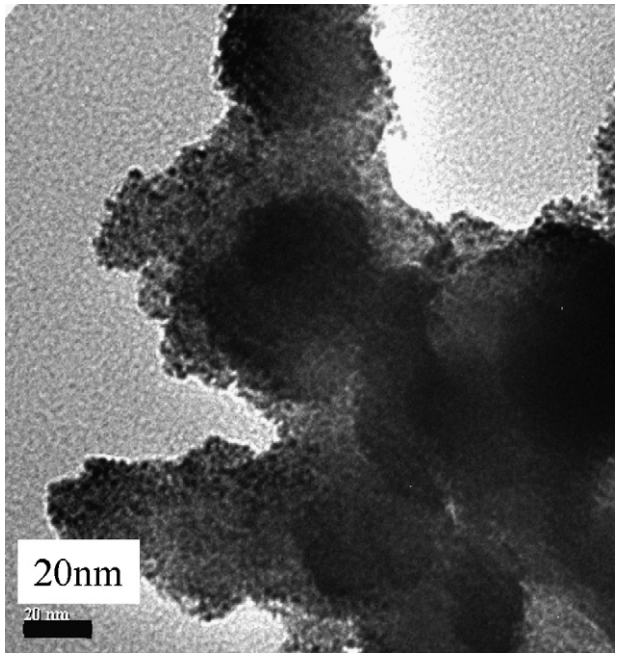

Fig. 1. TEM micrograph of Ir-Se chalcogenide powder.

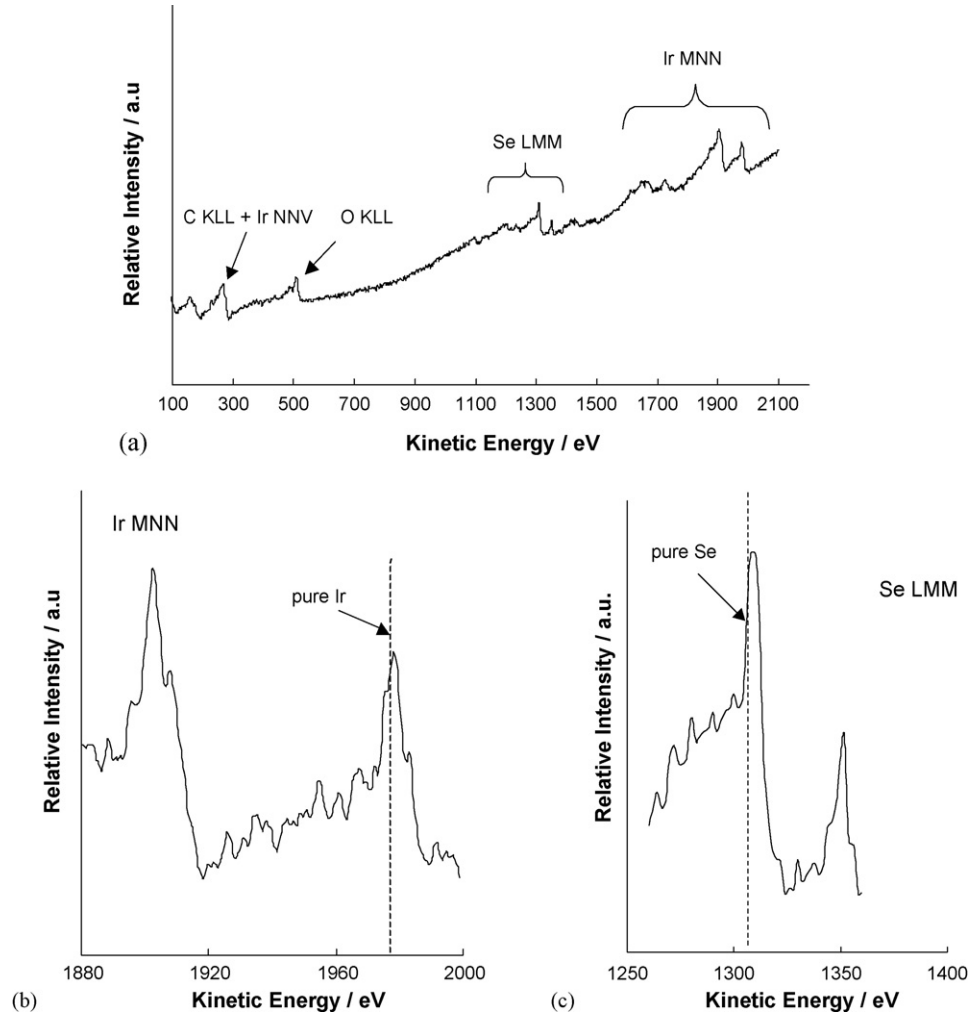

Fig. 2. Auger spectra for synthesized Ir-Se chalcogenide: (a) wide range spectrum, (b) Ir MNN spectrum, and (c) Se LMM spectrum.

chemical composition ratio of Se/Ir is 0.23. The sum content of carbon and oxygen are very low compared to those of Ir and Se, amounting to only 10.7% of total atomic composition. It is believed that this small amount of C + O was from the unreacted Ir carbonyl ($Ir_4(CO)_{12}$). According to the chemical stoichiometry of $Ir_4(CO)_{12}$, 10.7% carbonyl (CO) should bond with 3.6% Ir. Therefore, the atomic percentage of Ir in the total composition listed in Table 1 should be corrected by subtracting 3.6% from 72.7%, giving a corrected value of 69.1%. As a result, the chemical composition ratio of Se/Ir in the Ir-Se chalcogenide should be 0.24. Thus, the chemical formula for Ir-Se chalcogenide may be expressed as Ir_4Se. The weight purity of this Ir-Se chalcogenide powder is about 94.5 wt.%. Work on the purification of synthesized Ir-Se chalcogenide catalyst will be continued.

3.2. Cyclic voltammetric characterization

Fig. 3(a) shows the cyclic voltammograms (CVs) for Ir-Se chalcogenide catalyst in 0.5 M H_2SO_4 solutions with and without 0.5 M MeOH under N_2 atmosphere. The currents in Fig. 3 are expressed as apparent current densities (I_D) due to the electrode geometric area was used as the reaction area. For comparison, the CVs of a Ir/C catalyst are plotted in Fig. 3(b). In the absence of MeOH, the Ir-Se chalcogenide exhibited differ-

Table 1
Surface chemical composition Ir-Se chalcogenide by Auger electron spectroscopy

Element	Ir	Se	C	O	Se/Ir atomic ratio
Atomic% in the mixture of Ir-Se chalcogenide and Ir carbonyl	72.7	16.6	4.7	6.0	0.23
Atomic% in Ir-Se chalcogenide, corrected with respect to carbonyl content according to the stoichiometry of Ir in $Ir_4(CO)_{12}$	69.1	16.6	0	0	0.24

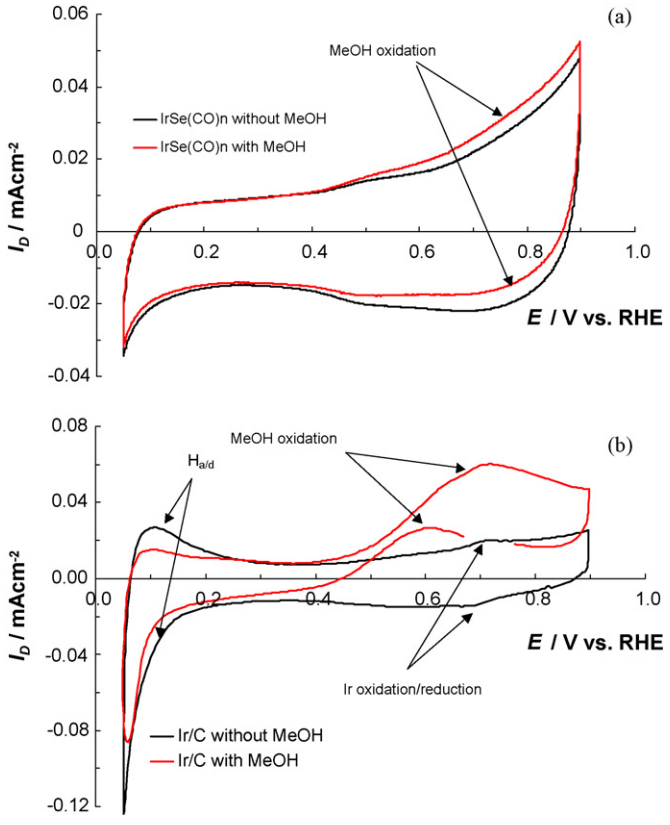

Fig. 3. Cyclic voltammograms for: (a) Ir-Se chalcogenide, and (b) Ir/C coated glassy carbon electrode in 0.5 M H_2SO_4 with and without 0.5 M MeOH under saturated N_2. Potential scan rate: 5 mVs^{-1}, 25 °C.

ent surface electrochemical behaviour from that of Ir/C. In the hydrogen adsorption/desorption ($H_{a/d}$) region, the Ir/C catalyst showed large $H_{a/d}$ peaks between 0.05 and 0.4 V versus RHE. Such hydrogen adsorption behaviour on the Ir/C catalyst agrees with that of the bare Ir electrode in the literature [5,9,10]. In contrast, the Ir-Se chalcogenide had no peaks corresponding to $H_{a/d}$ in the same potential region, indicating that the chemical adsorption state of hydrogen on the Ir sites bonded to Se is quite different from that of a pure Ir catalyst. The suppressed hydrogen adsorption peaks on Ir-Se chalcogenide might be due to the influence of the Se.

For the Ir/C catalyst, a reversible wave at 0.7 V versus RHE can be seen on the CV (Fig. 3(b)), which can be attributed to the Ir/IrOH or IrO redox process [5,9,10]. However, in the case of Ir-Se chalcogenide (Fig. 3(a)), no such redox waves corresponding to the formation of Ir oxide can be seen at the same potential, indicating that the formation of Ir oxide is suppressed. The small redox waves at approximately 0.5 V versus RHE in the CV of Ir-Se chalcogenide can be assigned to the hydroquinone-quinone redox couple of the glassy carbon disk electrode. From these results, it can be concluded that the presence of Se can effectively suppress the formation of Ir oxide.

In the presence of MeOH, the Ir/C catalyst showed catalytic activity towards MeOH oxidation, indicating that pure Ir is an active catalyst for methanol oxidation. In other words, Ir has no methanol tolerance properties. This observation of the Ir catalytic behaviour towards MeOH oxidation is consistent with the literature [7,8,10]. Aramata et al. reported that the reversible redox couple of Ir oxide formed at low potential range, below 0.8 V versus RHE, promoted MeOH oxidation in acidic electrolytes [10]. In the case of the Ir-Se chalcogenide catalyst, the catalytic activity towards methanol oxidation can be effectively reduced due to the fact that no surface Ir oxides are formed. As shown in Fig. 3(a), in the presence of methanol, the Ir-Se chalcogenide catalyst showed a quite similar CV to that without MeOH. This means that the Ir-Se chalcogenide catalyst has insignificant activity towards MeOH oxidation. It should be pointed out that the presence of Se in the Ir-Se chalcogenide catalyst plays a critical role in the MeOH tolerance because it prevents the formation of Ir oxides.

3.3. Electrocatalytic activity of Ir-Se chalcogenide catalyst towards ORR with/without MeOH

Fig. 4 shows the polarization curves of Ir-Se chalcogenide towards ORR in O_2-saturated 0.5 M H_2SO_4 solution with and without MeOH present. For comparison, the curves for Pt/C and Ir/C catalysts were also plotted. In the absence of MeOH, the Ir/C catalyst does not show a clear diffusion-limiting current at the overall applied potential range, while the Ir-Se chalcogenide has the diffusion-limiting region below 0.4 V versus RHE. This might suggest that the catalytic activity of Ir-Se chalcogenide is better than that of the Ir/C catalyst, but still lower than that of the Pt/C catalyst. In the presence of MeOH, the Pt/C and Ir/C catalysts show significant ORR performance drop compared to that when MeOH is absent, suggesting that both Pt/C and Ir/C have no methanol tolerance property. A large anodic current of Pt/C above 0.7 V is due to the MeOH oxidation. The ORR onset potential for catalyzed ORR by Pt/C is around 0.7 V versus RHE, which is over 300 mV lower than that when MeOH is absent. Such an ORR onset potential drop can be attributed to the mixed potential caused by the simultaneous reaction of O_2 reduction and MeOH oxidation. This observation clearly suggests that the Pt/C catalyst has no MeOH tolerance. For the Ir-Se chalcogenide, the open-circuit potential in saturated O_2 atmosphere was 0.93 V versus RHE in the absence of MeOH, and this value

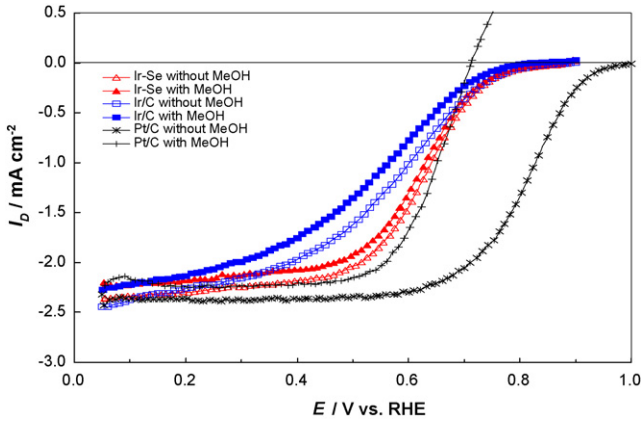

Fig. 4. Current–potential curves for Ir-Se chalcogenide, and Ir/C in 0.5 M H_2SO_4 with and without 0.5 M MeOH under saturated O_2. The current density is normalized to the geometric area. Potential scan rate: 400 rpm, 5 mVs^{-1}, 25 °C.

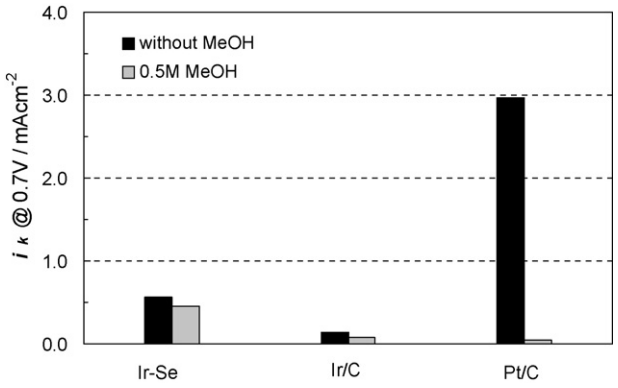

Fig. 5. Comparison of the kinetic current densities at 0.7 V vs. RHE normalized to the electrochemical active surface area.

was almost unchanged when MeOH was added into the electrolyte. The ORR performance was similar to that in the absence of MeOH, indicating that Ir-Se has a strong methanol tolerance property. In the presence of MeOH, the ORR onset potential of the Ir-Se chalcogenide is much higher (ca. 200 mV) than that of the Pt/C catalyst, demonstrating that Ir-Se chalcogenide has superior ORR performance to that of the Pt/C catalyst in terms of both ORR onset potential and current–potential performance (over 0.7 V versus RHE) in the presence of MeOH. These results suggest that the Ir-Se chalcogenide could be a promising catalyst for DMFC cathode.

Regarding the active catalytic site of the Ir-Se chalcogenide catalyst, Ir sites are believed to be responsible for the ORR [16]. The role of Se might be to enhance the ORR activity by modifying Ir sites. If Ir is the active site, the real active surface area of the Ir-Se chalcogenide catalyst might be deduced from the hydrogen adsorption/desorption peaks on the cyclic voltammogram by assuming that a monolayer of hydrogen adsorption on Ir corresponds to a charge of 220 μCcm^{-2} [17]. The kinetic current densities normalized with respect to the electrochemical active surface area were obtained from equation (1) [13]:

$$i_K = i\left(\frac{i_D}{i_D - i}\right) \quad (1)$$

where i_K is the kinetic current density for ORR, i the disk electrode current density, i_D is the diffusion-limiting current density. Fig. 5 compares the specific kinetic current densities at 0.7 V versus RHE with and without 0.5 M MeOH. The kinetic current densities were obtained based on the data in Fig. 4. In the absence of methanol, the Pt/C catalyst shows a specific activity ~6 times larger than that of the Ir-Se chalcogenide catalyst. However, in the presence of methanol, its activity is only ~1/10 of that of the Ir-Se catalyst.

Tafel plots for the kinetic current density normalized to the electrochemical active surface are shown in Fig. 6. Pt/C and Ir/C catalysts show two different Tafel regions with slopes of −60, and −120 mVdec.$^{-1}$, respectively. However, the Ir-Se chalcogenide has only one Tafel slope at −112 mVdec.$^{-1}$, indicating that this catalyst might have a similar ORR mechanism to those of oxide-free Pt and Ir catalyst [18,19].

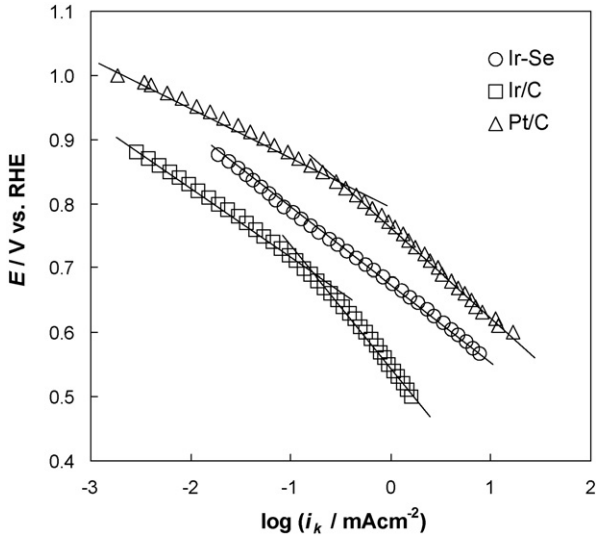

Fig. 6. Tafel plots for the ORR on Ir-Se chalcogenide, Ir/C and Pt/C without MeOH.

3.4. RRDE to detect H_2O_2

It is commonly recognized that the ORR in aqueous electrolyte may proceed by two overall pathways: the four-electron pathway in which the O_2 is reduced to water, and the peroxide pathway which produces hydrogen peroxide (H_2O_2) via a two-electron transfer process [20]. In order to gain insight into the kinetics and mechanism of the ORR catalyzed by the Ir-Se chalcogenide catalyst, the RRDE method was used to obtain the kinetic data and to identify the dominating pathway.

Fig. 7 shows the RRDE curves for catalyzed ORR at an electrode rotation rate of 400 rpm. The curve in the bottom portion of this figure is the disk currents (I_D) of catalyzed ORR and the curve in the upper portion is the ring currents (I_R) of the H_2O_2

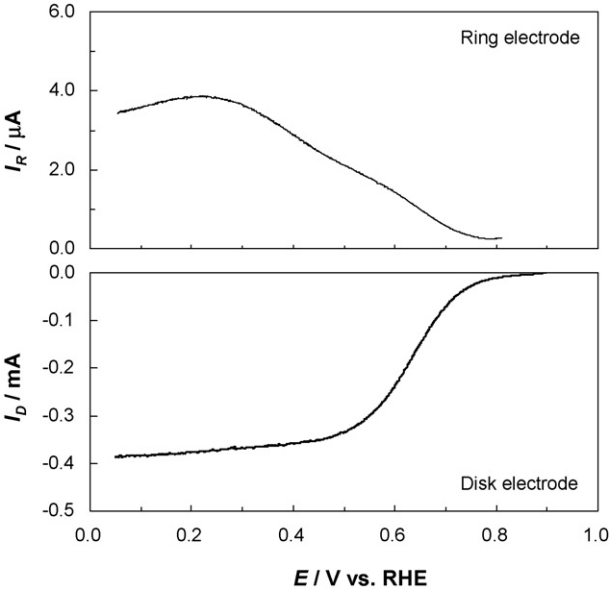

Fig. 7. RRDE curves of Ir-Se chalcogenide coated on glassy carbon disk-Pt ring electrode at an electrode rotation rate of 400 rpm in O_2 saturated 0.5 M H_2SO_4 solution. Potential scan rate: 5 mVs^{-1}. Ring electrode potential: 1.2 V vs. RHE.

oxidation. The H_2O_2 was produced by catalyzed ORR on the disk electrode, then thrown onto the ring by the electrode rating action. The percentage of the produced peroxide during disk ORR can be calculated by the following equation [13]

$$X\%_{H_2O_2} = \frac{200 I_R/N}{I_R/N + I_D} \quad (2)$$

where N is the collection efficiency (0.19 in this work). It was found that the average $X\%_{H_2O_2}$ is <10%, suggesting that more than 90% of the oxygen can be directly reduced to water. This result indicates that the catalyzed ORR by Ir-Se chalcogenide is dominated by a four-electron process.

4. Conclusions

A novel Ir-Se chalcogenide catalyst for oxygen reduction was synthesized by chemical reaction between an Ir carbonyl precursor and Se in an organic solvent. The catalyst was identified to have a chemical formula of Ir_4Se. This Ir-Se chalcogenide showed high catalytic activity towards the ORR with a strong MeOH tolerance. In particular, in the presence of methanol, this catalyst demonstrated an ORR performance superior to that of a Pt/C catalyst in terms of onset potential. Using a rotating ring-disk electrode (RRDE) technique we confirmed that less than 10% hydrogen peroxide was produced during the ORR. Most of the oxygen was directly reduced to water through a four-electron transfer pathway. The presence of Se is believed to play an important role in the enhanced ORR activity as a promoter via a bimetallic-like interaction, through which Se might suppress the formation of Ir-oxide.

Acknowledgements

This work is financially supported by the Institute for Fuel Cell Innovation, National Research Council of Canada (NRC-IFCI), and Natural Sciences and Engineering Research Council of Canada (NSERC).

References

[1] D. Chu, R. Jiang, Solid State Ionics 148 (2002) 591.
[2] L. Zhang, J. Zhang, D.P. Wilkinson, H. Wang, J. Power Sources 156 (2006) 171.
[3] K. Lee, O. Savadogo, A. Ishihara, S. Mitsushima, N. Kamiya, K.-I. Ota, J. Electrochem. Soc. 153 (2006) A20.
[4] M. Born, P. Bogdanoff, S. Fiechter, I. Dorbandt, M. Hilgendorff, H. Schulenburg, H. Tributsch, J. Electroanal. Chem. 500 (2001) 510.
[5] D.A.J. Rand, R. Woods, J. Electroanal. Chem. 55 (1974) 375.
[6] D.S. Gnanamuthu, J.V. Petrocelli, J. Electrochem. Soc. 114 (1967) 1036.
[7] M.W. Breiter, Electrochim. Acta 8 (1963) 973.
[8] V.S. Bagtzky, Yu.B. Vassiliev, O.A. Khazova, S.S. Sedova, Electrochim. Acta 16 (1971) 913.
[9] J. Mozota, B.E. Conway, Electrochim. Acta 28 (1983) 1.
[10] A. Aramata, T. Yamazaki, K. Kunimatsu, M. Enyo, J. Phys. Chem. 91 (1987) 2309.
[11] K.-I. Ota, A. Ishihara, S. Mitsushima, K. Lee, Y. Suzuki, N. Horibe, T. Nakagawa, N. Kamiya, J. New Mater. Electrochem. Syst. 8 (2005) 25.
[12] O. Solorza-Feria, K. Ellmer, M. Giersig, N. Alonso-Vante, Electrochim. Acta 39 (1994) 1647.
[13] U.A. Paulus, T.J. Schmidt, H.A. Gasteiger, R.J. Behm, J. Electroanal. Chem. 495 (2001) 134.
[14] J.D. Rogers, V.S. Sundaram, G.G. Kleiman, S.G.C. Castro, R.A. Douglas, A.C. Peterlevitz, J. Phys. F: Met. Phys. 12 (1982) 2097.
[15] M. Teo, P.C. Wong, L. Zhu, D. Susac, S.A. Campbell, K.A.R. Mitchell, R.R. Parsons, D. Bizzotto, Appl. Surface Sci. 253 (2006) 1130.
[16] D. Susac, A. Sode, L. Zhu, P.C. Wang, M. Teo, D. Bizzotto, K.A.R. Mitchell, R.R. Parsons, S.A. Campbell, J. Phys. Chem. B 110 (2006) 10762.
[17] B. Podlovchenko, G. Shterev, R. Semkov, E. Kolyadko, Electrochim. Acta 35 (1990) 191.
[18] D.B. Sepa, M.V. Vojnovic, Lj.M. Vracar, A. Damjanovic, Electrochim. Acta 32 (1987) 129.
[19] D.B. Sepa, M.V. Vojnovic, Lj.M. Vracar, A. Damjanovic, Electrochim. Acta 31 (1986) 91.
[20] K. Kinoshita, Electrochemical Oxygen Technology, John Willey & Sons, Inc., 1992, pp. 19.